ELSEVIER

Journal of Alloys and Compounds 356–357 (2003) 612–616

Journal of ALLOYS AND COMPOUNDS

www.elsevier.com/locate/jallcom

Phase structures and hydrogen storage properties of Ca–Mg–Ni alloys prepared by mechanical alloying

G. Liang*, R. Schulz

HERA Hydrogen Storage Systems Inc., 577 Le Breton, Longueuil, Quebec, Canada J4G 1R9

Received 1 June 2002; accepted 25 October 2002

Abstract

Binary Ca–Ni and ternary Ca–Mg–Ni alloys have been synthesized by mechanical alloying. The phase structures and hydrogen storage properties of the as-milled nanocrystalline and the thermally annealed alloys have been investigated. The phase structure changes with the (Ca+Mg)/Ni and the Mg/Ca ratios in the Ca–Mg–Ni ternary system. A too high Mg/Ca ratio leads to the formation of a $MgNi_2$ phase. The plateau pressure increases with Mg content in the $Ca_xMg_{1-x}Ni_2$ and $Ca_xMg_{1-x}Ni_3$ pseudo-binary alloys, however, the hydrogen storage capacity decreases. Mg does not substitute Ca in the $CaNi_5$ and Ca_2Ni_7 compounds. Adding or substituting a small amount of Mg in these compounds destroys the A_2B_7 as well as the AB_5 structures and results in an AB_3 phase and an accompanying nickel phase.

Keywords: Mechanical alloying; Nanostructure; Hydrogen absorbing alloys; Ca–Ni alloy

1. Introduction

Calcium–nickel-based alloys are potential low-cost hydrogen storage materials. In the Ca–Ni system, four stable compounds $CaNi_2$, $CaNi_3$, Ca_2Ni_7 and $CaNi_5$ were reported [1]. Among them, only the $CaNi_5$ was considered to be of practical interest for hydrogen storage since the plateau pressures of $CaNi_5$ are adequate for applications [2]. The other three compounds do form very stable hydrides. Hydrogen cannot be extracted at temperatures below 100 °C under normal pressure [3].

$CaNi_5$ has a maximum hydrogen storage capacity of 1.9 wt.% [2,4,5], but a bad cycling stability [6]. Improvement of the hydrogen storage properties of $CaNi_5$ by substituting Ca and/or Ni with some other elements has been tried [4,5,7–9]. The substitution of Mg for Ca in the $CaNi_5$ structure by liquid phase sintering of a mixture of Ca, Mg and Ni elements was not successful, the $Ca_{1-x}Mg_xNi_5$ alloy appears not to extend homogeneously beyond $x=0.06$ as reported by Oesterreicher et al. [7].

Mg can substitute Ca or La atoms in the ANi_2 and ANi_3 compounds (A=Ca, La) to form $A_{1-x}Mg_xNi_2$ and $A_{1-x}Mg_xNi_3$ pseudo-binary alloys up to $x=0.67$ [7,10,11]. A $Ca_{0.5}Mg_{0.5}Ni_2$ alloy was synthesized by liquid phase sintering of Ca, Mg and Ni elements in a Ta tube [7]. Recent work shows that the pseudo-binary $Ca_xMg_{1-x}Ni_2$ alloys with a C15 structure can be made by melt casting for $x \geq 0.33$ [11].

In the AB_3 pseudo-binary system, a $CaMg_2Ni_9$ compound of the $PuNi_3$ structure was synthesized by sintering powder mixtures of $MgNi_2$ and $CaNi_5$ or elemental Mg, Ca and Ni powder mixtures in a Mo crucible for a long time [10]. In this work, we synthesize binary Ca–Ni and ternary Ca–Mg–Ni alloys by mechanical alloying at room temperature, followed by an annealing treatment at elevated temperatures for a short time. The phase structure and the hydrogen storage properties of the mechanically alloyed and the thermally treated alloys have been investigated.

2. Experimental

Commercial grade Ca (1–2 mm in diameter), Ni (−325 mesh) and Mg (−100 mesh) powders were used as raw materials. Mechanical alloying was performed on a Spex 8000 ball mill at room temperature. The powders were mixed in the desired composition and mechanically milled for 40 h in a steel milling vial filled with argon. Three steel

*Corresponding author. Fax: +1-450-651-3801.
E-mail address: gl@herahydrogen.com (G. Liang).

0925-8388/02/$ – see front matter
doi:10.1016/S0925-8388(02)01285-9

balls of a diameter of 11 mm were used. The ball to powder mass ratio was 10:1. All the handling was performed in a glove-box.

The as-milled powder was placed in a tubular furnace for isothermal annealing treatment under the protection of flowing argon. The annealing conditions were fixed at 1050 °C for 1 h for all alloys except AB_2 type, where the annealing temperature is 1000 °C.

The hydrogen storage properties were evaluated by using an automated Sievert's apparatus. The X-ray powder diffraction (XRD) was performed on a Siemens D500 apparatus with Cu Kα radiation. The lattice parameters were determined from diffraction peak positions. The crystallite size was evaluated from the broadening of X-ray diffraction peaks using the Williamson–Hall method [12]. The peak position and peak broadening were calibrated by using strain free pure Si powders.

3. Results and discussion

3.1. Binary Ca–Ni system

Fig. 1 shows the XRD spectra of various Ca–Ni alloys made by mechanical alloying. Nanocrystalline $CaNi_2$ and $CaNi_3$ compounds are obtained by mechanical alloying of the elemental Ca and Ni powder blends at room temperature. The crystallite sizes of both compounds are estimated to be about 8 nm by using the Williamson–Hall method. At the Ca_2Ni_7 composition, a multiphase mixture of Ca_2Ni_7, $CaNi_3$ and possibly some nickel is obtained. Since the diffraction peaks of various phases overlap with each other, it is difficult to determine the crystallite size and abundance of each single phase by X-ray analysis. The $CaCu_5$ structure does not form at the stoichiometric $CaNi_5$ composition after mechanical alloying, strong Ni peaks are still present after 70 h of milling [9].

Both of the mechanically alloyed $CaNi_2$ and $CaNi_3$ can absorb more than 2 wt.% of hydrogen at room temperature without activation. However, no hydrogen can be released at temperatures below 100 °C under normal pressure. Some hydrogen can be released by heating to 200 °C.

The mechanically alloyed $CaNi_5$ crystallizes in the $CaCu_5$ structure after thermal annealing at 1050 °C. The $CaNi_5$ compound thus made can absorb/desorb hydrogen reversibly at 30 °C with a desorption plateau pressure of 0.05 MPa. For the Ca_2Ni_7 case, a mixture of Ca_2Ni_7, $CaNi_5$ and Ni phases is obtained after annealing treatment. The hydrogen storage properties of this mixture has not been investigated.

3.2. Synthesis of ternary Ca–Mg–Ni alloys

Mechanical alloying of the $Ca_xMg_{1-x}Ni_2$ pseudo-binary alloys leads to a cubic C15 nanocrystalline structure for $x \geq 0.3$. A representative XRD spectrum is shown in Fig. 2 for the $Ca_{0.4}Mg_{0.6}Ni_2$ alloy. An amorphous phase is obtained at the $Ca_{0.2}Mg_{0.8}Ni_2$ composition (not shown). Further increase of the Mg content leads to a predominant $MgNi_2$ type phase with C36 structure when the mechanical alloying process reaches a steady state.

In the pseudo-binary $Ca_xMg_{1-x}Ni_3$ system, a

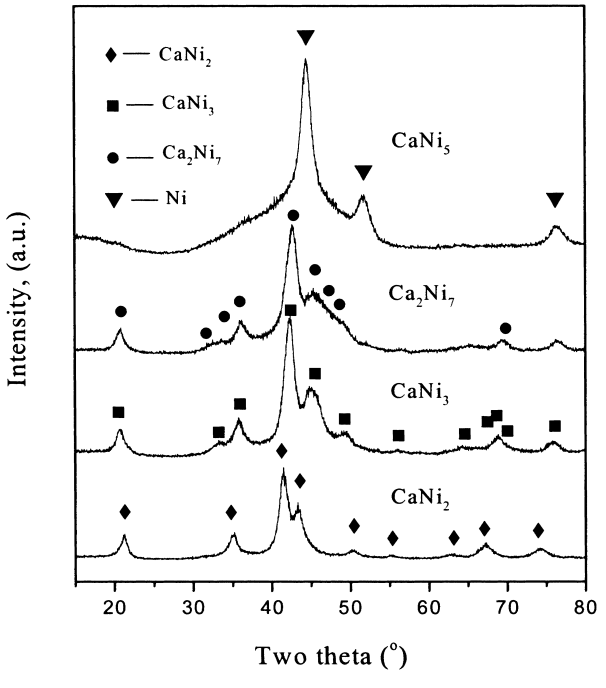

Fig. 1. XRD spectra of various Ca–Ni alloys made by mechanical alloying for 40 h.

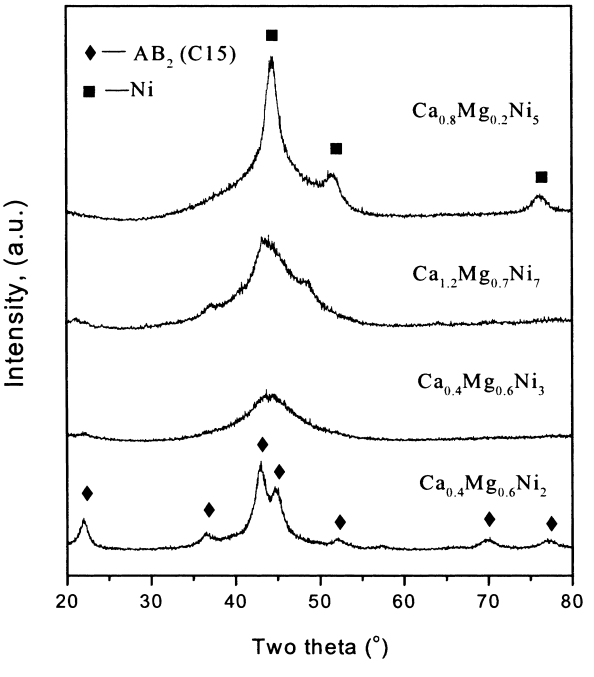

Fig. 2. XRD spectra of various Ca–Mg–Ni ternary alloys made by mechanical alloying for 40 h.

nanocrystalline AB_3 type phase with $PuNi_3$ structure forms for $x \geq 0.5$. The lattice parameters of the $PuNi_3$ type phase are reduced by substituting Ca with Mg. An amorphous-like phase is obtained for $Ca_{0.4}Mg_{0.6}Ni_3$ (see Fig. 2) and $Ca_{0.33}Mg_{0.67}Ni_3$ (not shown).

Substituting Mg for Ca in $CaNi_5$ does not lead to the formation of the AB_5 structure by mechanical alloying. The mechanically alloyed $Ca_{0.8}Mg_{0.2}Ni_5$ shows strong nickel peaks and a halo peak (see Fig. 2), suggesting that an amorphous phase is formed besides the nanocrystalline nickel phase.

A mixture of nanocrystalline AB_3, A_2B_7, and probably some Ni are obtained for Ca–Mg–Ni alloys having compositions at or close to A_2B_7. Since the diffraction peaks are very broad and they overlap with each other, it is difficult to determine whether Mg is substituted in the A_2B_7 and AB_5 by mechanical alloying. Table 1 summarize the phase structures obtained by mechanical alloying at various compositions.

Thermal annealing of the mechanically alloyed powders leads to grain growth, release of microstrain and changes of phase structure. If the alloying elements are not homogeneous after mechanical alloying, some intermediate phases such as $CaMg_2$, $MgNi_2$ and even Ni may be present in the end products when the annealing time is short and the annealing temperature is low, because an equilibrium state has not been reached. Long time of mechanical alloying or annealing treatment can get rid of those intermediate phases.

In the equilibrium state, the phase structure changes with the Mg, Ca and Ni contents. As shown in Fig. 3, when keeping the Mg/Ca ratio at 1.5, the structure of the end products changes with the (Ca+Mg)/Ni ratio. An AB_2 type phase is obtained for the $Ca_{0.4}Mg_{0.6}Ni_2$ with a (Ca+Mg)/Ni ratio of 0.5. Reducing the (Ca+Mg)/Ni ratio to 0.35, an AB_3 phase forms. The formation range of the AB_2 and AB_3 phases also changes with the Mg/Ca ratio. If Mg/Ca≥1.8, a second phase of $MgNi_2$ starts to form in the AB_3 system. This ratio should be smaller than 2.3 for preventing the formation of the $MgNi_2$ phase in the AB_2 system.

Mg cannot substitute Ca in the Ca_2Ni_7 and $CaNi_5$ structures under equilibrium conditions. As shown in Fig. 3, the mechanically alloyed $Ca_{0.8}Mg_{0.2}Ni_5$ crystallizes in the AB_3 ($PuNi_3$) structure, and the excess nickel is liberated as pure element after the thermal annealing treatment. When excess Ca is added in the $CaNi_5$, for example, in the composition of $CaNi_4$, a second Ca_2Ni_7 phase forms. However, in the case of Mg–Ca–Ni alloys, no AB_5 and A_2B_7 structures are observed in the composition range of (Ca+Mg)/Ni=0.33–0.2. All the alloys crystallize in the AB_3 structure with an accompanying nickel phase. Another example is for $Ca_{1.2}Mg_{0.7}Ni_7$ alloy which has a composition close to A_2B_7, a mixture of AB_3 and free nickel is obtained after annealing. Table 2 summarizes the phase structures observed at various compositions after thermal annealing.

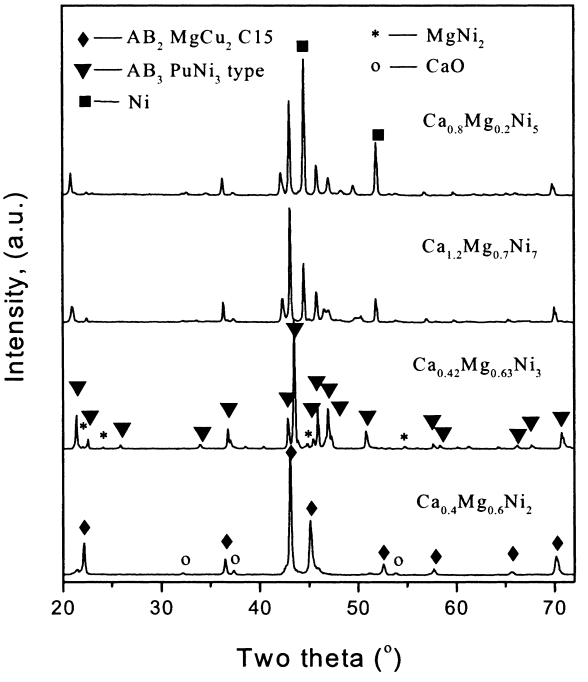

Fig. 3. XRD spectra of some Ca–Mg–Ni alloys made by mechanical alloying followed by annealing treatment.

3.3. Hydrogen storage properties of ternary Ca–Mg–Ni alloys

The as-milled nanocrystalline $Ca_xMg_{1-x}Ni_2$ and $Ca_xMg_{1-x}Ni_3$ alloys absorb hydrogen but with bad re-

Table 1
Phase structures observed at various compositions after mechanical alloying

Alloy system	Phase structures at steady state		
$Ca_xMg_{1-x}Ni_2$	$MgCu_2$ type C15 structure for $x \geq 0.3$	Amorphous-like phase at $x=0.2$	$MgNi_2$ type C36 structure for $x \leq 0.2$
$Ca_xMg_{1-x}Ni_3$	$PuNi_3$ type phase for $x \geq 0.5$	Amorphous-like phase for $x=0.33$–0.4	$x<0.33$, not investigated
$Ca_xMg_{2-x}Ni_7$	$A_2B_7+AB_3+Ni$ for $2>x \geq 1.2$	Not investigated for $x<1.2$	
$Ca_xMg_{1-x}Ni_5$	Nano-Ni+amorphous phase for $1>x \geq 0.8$	Not investigated for $x<0.8$	

Table 2
Phase structures observed at various compositions after thermal annealing

Alloy system	Phase structures in the equilibrium state		
$Ca_xMg_{1-x}Ni_2$	C15 type phase for $x \geq 0.3$	C15+C36 for $x=0.2$	Not investigated for $x<0.2$
$Ca_xMg_{1-x}Ni_3$	$PuNi_3$ type phase for $x \geq 0.5$	AB_3+C36 (minor) for $0.33<x<0.4$	Not investigated for $x<0.33$
$Ca_xMg_{2-x}Ni_7$	AB_3+Ni For $2>x \geq 1.2$; $A_2B_7+AB_5$+Ni for $x=2$	Not investigated for $x<1.2$	
$Ca_xMg_{1-x}Ni_5$	AB_3+Ni for $1>x \geq 0.8$; AB_5 for $x=1$	Not investigated for $x<0.8$	

versibility due to their particular structure. For example, the $Ca_{0.5}Mg_{0.5}Ni_3$ alloy absorbs 1.4 wt.% of hydrogen at room temperature under 3.0 MPa of hydrogen pressure; however, only 0.85 wt.% of hydrogen can be released at the same temperature under vacuum. This is a common feature of mechanically alloyed nanocrystalline and amorphous alloys [13]. Annealing treatment leads to grain growth, release of microstrain and reordering of atoms, and therefore, to an increase of the reversible storage capacity [14].

Fig. 4 shows the PCT curves of various Ca–Mg–Ni alloys after thermal annealing. In the case of the AB_2 alloy, an inclined plateau with steep slope is obtained for $Ca_{0.4}Mg_{0.6}Ni_2$. We observe that the $Ca_{0.8}Mg_{0.2}Ni_5$ has a lower plateau pressure than that of $CaNi_5$. This is because the $Ca_{0.8}Mg_{0.2}Ni_5$ separates into $Ca_{0.8}Mg_{0.2}Ni_3$+2Ni upon annealing treatment and the Ca-rich $Ca_{0.8}Mg_{0.2}Ni_3$ alloy has a lower plateau pressure than that of $CaNi_5$. For the $Ca_{1.2}Mg_{0.7}Ni_7$ case, a mixture of $Ca_{0.63}Mg_{0.37}Ni_3$+1.3Ni is obtained. The $Ca_{0.63}Mg_{0.37}Ni_3$ has a slightly higher plateau pressure than that of $CaNi_5$.

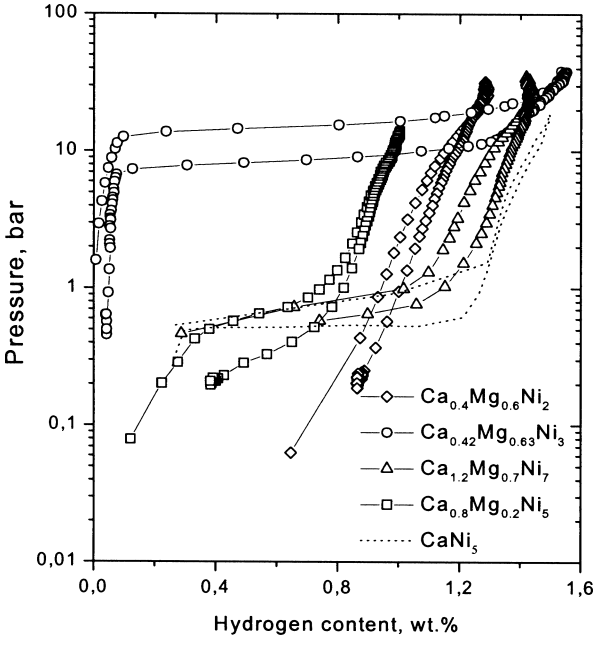

Fig. 4. PCT curves at 30 °C of selected Ca–Mg–Ni alloys after thermal annealing.

The hydrogen storage capacities of the C15 type $Ca_{0.4}Mg_{0.6}Ni_2$ alloy is about 2H per formula unit (2H/f.u.). This is much lower than the reported values for C15 type ZrV_2 (5.2H/f.u.) and $ZrCr_2$ (3.4H/f.u.) [15]. The small hydrogen storage capacity could be due to the small unit cell volume of the $Ca_xMg_{1-x}Ni_2$ alloys because the size of the interstitial holes becomes smaller with decreasing the lattice parameter. For example, the lattice parameter of the $Ca_{0.4}Mg_{0.6}Ni_2$ alloy is measured to be 0.6965 nm, therefore, the interstitial hole radius for the A_2B_2 site (the largest hole in this C15 structure) is only 0.037 nm. If the volume expansion is about 17% upon hydrogenation as measured in [11], the hole radius of the A_2B_2 site in the hydride is 0.043 nm, which is just slightly larger than 0.04 nm, the critical minimum hole radius for holding a hydrogen atom [15]. However, the other interstitial holes are too small to let H atom in. One possible way to increase the storage capacity of the $Ca_xMg_{1-x}Ni_2$ system is to increase the unit cell volume through substitution. The hydrogen storage capacity increases from 2H/f.u. at $x=0.4$ to 3.4H/f.u. at $x=1$. However, the reversibility decreases significantly.

The $Ca_{0.42}Mg_{0.63}Ni_3$ alloy has a hydrogen storage capacity of 1.56 wt.% (about 2.7H/f.u.). The AB_3 type alloy is generally considered as a superstructure (long range stacking arrangement) containing one-third of AB_5 layer and two-thirds of AB_2 layer [16]. The maximum hydrogen storage capacity of AB_5 is 6H/f.u., while that of Mg-rich Ca–Mg–Ni AB_2 type alloy is about 2H/f.u., therefore, the hydrogen storage capacity of the Mg-rich AB_3 type Ca–Mg–Ni alloys is about 3.3H/f.u. This is close to that observed in the $Ca_{0.42}Mg_{0.63}Ni_3$ alloy. The formation of minor $MgNi_2$ phase causes additional loss of storage capacity. The hydrogen storage capacity does increase with Ca content in $Ca_xMg_{1-x}Ni_3$ and to 4.5H/f.u. for $CaNi_3$.

4. Conclusions

(1) Mechanical alloying of elemental Ca, Mg and Ni powder blends leads to nanocrystalline $Ca_xMg_{1-x}Ni_2$ and $Ca_xMg_{1-x}Ni_3$ pseudo-binary alloys in the Ca-rich side. The lattice parameters decrease with Mg content.
(2) Substituting or adding a small amount of Mg in Ca_2Ni_7 or $CaNi_5$ destroys the A_2B_7 as well as the AB_5 structures and results in an AB_3 phase with an accompanying nickel phase in the composition range of AB_3 and AB_5.
(3) The as-milled nanocrystalline $Ca_xMg_{1-x}Ni_2$ and $Ca_xMg_{1-x}Ni_3$ absorbs hydrogen with bad reversibility. Thermal annealing treatment improves the reversibility and enhance the hydrogen storage capacity. The plateau pressure increases and the reversible hydrogen storage capacity decreases with the Mg content.

References

[1] T.B. Massalski, in: Binary Alloy Phase Diagram, ASM International, Metals Park, OH, 1991.
[2] G.D. Sandrock, Proc. 12th Intersociety Energy Conversion Engineering Conference, Am. Nuclear Soc. 1 (1977) 951.
[3] G. Sandrock, G. Thomas, IEA technical report, compilation of IEA/DOE/SNL hydride database, 1997.
[4] G.D. Sandrock, in: A.F. Andersen, A.J. Maeland (Eds.), Proc. Int. Symp. on Hydrides for Energy Storage 9, Pergamon, Oxford, 1978, p. 1625.
[5] G.D. Sandrock, J.J. Murray, M.L. Post, J.B. Taylor, Mater. Res. Bull. 17 (1982) 887.
[6] P.D. Goodell, J. Less-Common Met. 99 (1984) 1.
[7] H. Oesterreicher, K. Ensslen, A. Kerlin, E. Bucher, Mater. Res. Bull. 15 (1980) 275.
[8] J.O. Jensen, N.J. Bjerrum, J. Alloys Comp. 293–295 (1999) 185.
[9] G. Liang, J. Huot, R. Schulz, J. Alloys Comp. 321 (2001) 146–150.
[10] K. Kadir, N. Kuriyama, T. Sakai, I. Uehara, L. Eriksson, J. Alloys Comp. 284 (1999) 145.
[11] N. Terashita, K. Kobayashi, T. Sasai, E. Akiba, J. Alloys Comp. 327 (2001) 275.
[12] H.P. Klug, L. Alexander, in: X-ray Diffraction Procedures for Polycrystalline and Amorphous Materials, 2nd Edition, Wiley, New York, 1974, pp. 619–708.
[13] G. Liang, R. Schulz, Mater. Trans. JIM 42 (2001) 1593.
[14] G. Liang, R. Schulz, in: Proc. of 14th WHEC, June 9–13, 2002, Montreal, Canada, 2002.
[15] D.G. Westlake, J. Less-Common Met. 90 (1983) 251.
[16] B.D. Dunlap, P.J. Viccaro, G.K. Shenoy, J. Less-Common Met. 74 (1980) 75.